



Published in final edited form as:

*Angew Chem Int Ed Engl.* 2009 ; 48(27): 4996–5000. doi:10.1002/anie.200805940.

## Dynamic Nuclear Polarization using a Rigid Biradical\*\*

### Dr. Yoh Matsuki,

Francis Bitter Magnet Laboratory and Department of Chemistry, Massachusetts Institute of Technology, Cambridge MA 02139 (USA)

Department of Chemistry, Brandeis University, Waltham MA 02454 (USA)

### Dr. Thorsten Maly,

Francis Bitter Magnet Laboratory and Department of Chemistry, Massachusetts Institute of Technology, Cambridge MA 02139 (USA)

### Dr. Olivier Ouari,

CNRS-UMR 6517, Chemistry, Biology and Free Radicals, University of Aix-Marseille I et III, Marseille (France)

### Dr. Hakim Karoui,

LCP CNRS-UMR 6264, University de Provence, 13397 Marseilles Cedex 20 (France)

### Dr. François Le Moigne,

LCP CNRS-UMR 6264, University de Provence, 13397 Marseilles Cedex 20 (France)

### Dr. Egon Rizzato,

LCP CNRS-UMR 6264, University de Provence, 13397 Marseilles Cedex 20 (France)

### Dr. Sevdalina Lyubenova,

Institute of Physical and Theoretical Chemistry and Center for Biomolecular Magnetic Resonance, 60438 Frankfurt (Germany)

### Judith Herzfeld[Prof.],

Department of Chemistry, Brandeis University, Waltham MA 02454 (USA)

### Thomas Prisner[Prof.],

Institute of Physical and Theoretical Chemistry and Center for Biomolecular Magnetic Resonance, 60438 Frankfurt (Germany)

### Paul Tordo[Prof.], and

CNRS-UMR 6517, Chemistry, Biology and Free Radicals, University of Aix-Marseille I et III, Marseille (France)

### Robert G. Griffin\* [Prof.]

Francis Bitter Magnet Laboratory and Department of Chemistry, Massachusetts Institute of Technology, Cambridge MA 02139 (USA)

\*\*The authors thank Sandrine Lambert for technical assistance, Galia Debelouchina, Albert Smith, Alexander Barnes and Jean-Pierre Finet for many stimulating discussions. This research was supported by the National Institutes of Health through grants EB002804, EB002026, EB009866, EB001965 and EB001035 and by the EU-Design Study Bio-DNP in Framework 6. T.M. acknowledges receipt of a postdoctoral fellowship of the Deutsche Forschungs Gemeinschaft. Y.M. acknowledges partial financial support from the Naito foundation.

\*Fax: (+1) 781 736 2538, rgg@mit.edu, Homepage: <http://web.mit.edu/fbml/cmr/griffin-group/index.html>.

Supporting information for this article is available on the WWW under <http://www.angewandte.org> or from the author.

## Keywords

DNP; solid-state NMR; polarizing agents; biradicals

Dynamic nuclear polarization (DNP) is an approach that can enhance NMR signal intensities of solids and liquids by two to three orders of magnitude. During a DNP experiment, the large Boltzmann polarization of an exogenous or endogenous paramagnetic species, such as a stable free radical, is transferred to the nuclei of interest by microwave (mw) irradiation of the sample at the electron paramagnetic resonance (EPR) frequency. The maximum theoretical enhancement achievable is given by the ratio  $\gamma_s/\gamma_I$ , where  $\gamma_s$  and  $\gamma_I$  are the gyromagnetic ratios of the electron and the nucleus, respectively. The enhanced nuclear polarization is of considerable interest in a variety of applications ranging from particle physics [1,2] to structural biology [3,4] and clinical imaging.[5] The mechanism that dominates the electron-nuclear polarization transfer depends on the relative sizes of the homogeneous linewidth,  $\delta$ , and the inhomogeneous breadth,  $\Delta$  of the EPR spectrum of the paramagnetic polarizing agent compared to the nuclear Larmor frequency,  $\omega_{0I}$ . When  $\delta, \Delta < \omega_{0I}$  DNP is dominated by the solid-effect (SE), whereas when  $\Delta > \omega_{0I} > \delta$  the cross-effect (CE) is operative.[3] In general, the largest signal enhancements observed at high magnetic fields ( $\geq 5$  T) are in experiments where the CE controls the polarization transfer.[6,7] The underlying mechanism of the CE is a two-step process that involving two electrons with Larmor frequencies  $\omega_{0S1}$  and  $\omega_{0S2}$  and a nucleus with a frequency  $\omega_{0I}$ . Initially, the EPR transition of one electron is irradiated and then nuclear polarization is generated in a subsequent three-spin flip-flop process through transitions such as  $|\alpha_{1S}\beta_{2S}\beta_I\rangle \leftrightarrow |\beta_{1S}\alpha_{2S}\alpha_I\rangle$  or  $|\beta_{1S}\alpha_{2S}\beta_I\rangle \leftrightarrow |\alpha_{1S}\beta_{2S}\alpha_I\rangle$ . [8–10] Therefore, the CE is optimized when there is a sufficiently strong dipolar coupling between the two electrons, and the difference between the electron Larmor frequencies approximates the nuclear Larmor frequency ( $\omega_{0S1} - \omega_{0S2} \approx \pm \omega_{0I}$ ). These requirements can be more easily fulfilled within a biradical than among dispersed monoradicals,[11] and we have demonstrated that the optimal polarizing agent for experiments in glycerol/water is currently the TEMPO based biradical 1-(TEMPO-4-oxy)-3-(TEMPO-4-amino)propan-2-ol (TOTAPOL) [12] (Figure 1, bottom). However, at high magnetic fields the effective electron resonance frequency can depend strongly on the molecular orientation with respect to the external magnetic field, and in a biradical the matching condition is controlled by the relative orientations of the electron g-tensors. In particular, since the propan-2-ol tether in TOTAPOL is relatively flexible,[6] the relative orientation of the two TEMPO moieties is not well constrained and many orientations do not lead to the correct frequency separation. Therefore, a more rigid tether that locks the two TEMPO moieties at a desirable relative orientation should further increase the enhancement obtained from the polarizing agent.

In this report we demonstrate the utility of bis-TEMPO-bis-ketal (bTbk) (Figure 1, top), a biradical consisting of two TEMPO moieties connected with a rigid bis-ketal tether that was originally used to inhibit radical polymerization.[13] In particular we compare and characterized the performance of bTbk and TOTAPOL in DNP experiments under similar experimental conditions.

Earlier studies of a series of TEMPO-based biradicals as polarizing agents in high-field DNP experiments suggested that a conformation in which the two  $g_{zz}$  (or  $g_{yy}$ ) tensor axes of the TEMPO moieties have a dihedral angle of  $90^\circ$  should exhibit improved performance due to efficient frequency matching [6]. This requirement is approximately fulfilled (*vide infra*) for bTbk (Figure 1, top) due to the odd number of spiranic junctions between the two TEMPO moieties. Specifically, the crystal structure of bTbk shows a dihedral angle between the TEMPO moieties of  $82^\circ$ . Furthermore a calculated average electron-electron distance of

1.18 nm (Figure S1, supporting information) has been confirmed by PELDOR measurements (Figure S2, supporting information). The dihedral angle restrains the  $g_{zz}$  (or  $g_{yy}$ ) tensor components of the two TEMPO moieties in a perpendicular conformation, ensuring a large frequency separation for molecular orientations along these axes. At the same time the short distance provides the large electron-electron dipolar coupling required for an efficient DNP process.

Initial DNP experiments using bTbk are presented in Figure 2. A typical  $^{13}\text{C}$  detected  $^1\text{H}$  bulk polarization build-up curve is shown together with spectra recorded with and without microwave irradiation at fields corresponding to the maximum positive (DNP(+)) and negative (DNP(-)) DNP enhancements (using the pulse sequence given in Figure S3, supporting information). Here, the  $^1\text{H}$  polarization is monitored by transferring the DNP-enhanced  $^1\text{H}$  polarization to the  $^{13}\text{C}$  nuclei of the urea molecule in a cross-polarization step. [14,15] At a temperature of 93 K, the build-up time constant  $\tau_B$  is 7 s, and a steady state enhancement of  $\varepsilon^+ = 250$  was observed (Figure 2) at a microwave power of  $\sim 2.5$  W (estimated power at the sample position). This enhancement is larger than that of TOTAPOL ( $\varepsilon^+ = 180$ ), observed under identical experimental conditions (solvent, temperature, mw power).

A more reliable comparison between the two polarizing agents can be achieved by comparing the enhancement extrapolated to infinite microwave power  $\varepsilon_\infty^\pm$ . This value can be obtained from the microwave power dependence of the DNP enhancement given by

$$\frac{1}{\varepsilon^\pm} = \frac{1}{\varepsilon_\infty^\pm} \left( 1 + \frac{1}{aP} \right), \quad (1)$$

with  $\varepsilon^\pm$  the steady-state enhancement factor,  $P$  the microwave power, and  $a$  the saturation parameter, which depends on the microwave transmission efficiency and EPR relaxation properties [6]. Here different instrumental conditions such as the microwave transmission efficiency or EPR relaxation properties only affect  $\varepsilon^\pm$  and  $a$  but not  $\varepsilon_\infty^\pm$ . [6] Nevertheless, the experiments must be performed at similar temperatures for an accurate comparison.

Figure 3 shows the power dependence of the DNP enhancements for bTbk and TOTAPOL from which  $\varepsilon_\infty^\pm$  can be calculated using equation (1). For bTbk and TOTAPOL, the  $\varepsilon_\infty^+$  values are  $325 \pm 15$  and  $227 \pm 10$ , respectively. In Table 1 values of  $\varepsilon_\infty^+$  for a series of biradicals previously examined in DNP experiments are compared. Among the polarizing agents investigated to-date, bTbk yields the largest DNP enhancements, approximately 1.4 times larger than that of TOTAPOL.

The DNP process is most efficient if the sample and the polarizing agent are dispersed in a matrix that forms a rigid glass at cryogenic temperatures. For example, mixtures of DMSO/water (60/40 weight/weight) or glycerol/water (60/40 weight/weight) form rigid glass matrices at 90 K regardless of the cooling rate. [3,4,16,17] The ability of the solvent to form a glass is important in DNP experiments, because it ensures a homogeneous dispersion of the polarizing agent in the sample, and it can concurrently acts as a cryoprotectant. However, in the case of bTbk the main factor presently limiting its applicability in DNP experiments to biological samples is its sparse solubility in media such as glycerol/water (60/40), which is currently the solvent of choice for DNP experiments on proteins. While small amounts of bTbk are soluble in 60/40 DMSO/water, another mixture used frequently for DNP, the solubility is greater at higher DMSO concentrations. However, DMSO requires a minimum water content of 23 % for successful glass formation at 90 K. Therefore, all experiments reported here were performed using a 77/23 DMSO/water mixture.

The reduced water content has a dramatic impact on the observed enhancements. In measurements of  $\varepsilon_{\infty}^+$  for TOTAPOL in different solvent matrices with a DMSO content of 50, 64 and 77 % we observed that  $\varepsilon_{\infty}^+$  for 50/50 and 64/36 mixtures of DMSO/water are similar ( $\varepsilon_{\infty}^+ \sim 260$ ), while the observed enhancement is significantly lower at a water content of 23 % ( $\varepsilon_{\infty}^+ \sim 230$ , see Table 1). This decrease is most likely due to the suboptimal glass forming properties of the 77/23 DMSO/water mixture. Nevertheless in this solvent matrix a maximum enhancement of  $\varepsilon_{\infty}^+ = 325$  was observed for bTbk: an increase by 40 % if the performance is compared under identical experimental conditions ( $\varepsilon_{\infty}^+ = 230$  for TOTAPOL). If  $\varepsilon_{\infty}^+$  is compared under optimal conditions for bTbk and TOTAPOL, then the increase is 25% ( $\varepsilon_{\infty}^+ = 260$  for TOTAPOL in DMSO/water 60/40). Taken together, these results suggest that still greater DNP enhancements can be expected for a water-soluble form of bTbk.

Since the gyrotron is a fixed frequency oscillator (operating at 139.662 GHz), the optimum field position for the DNP effect is determined by sweeping the magnetic field,  $B_0$ , and recording the DNP enhancement for each field position. This yields the field-dependent DNP enhancement profile illustrated in Figure 4 (bottom). Besides identifying the fields for maximum enhancements (DNP(+)) and DNP(-), the DNP profile provides other important information that can lead to possible improvements of the performance of the polarizing agent.

The DNP enhancement profile is closely related to the high-field EPR spectrum, which is shown for bTbk in Figure 4 (top). Since the electron-electron dipolar coupling is relatively small ( $\sim 30$  MHz) compared to the breadth of the EPR spectrum, the lineshape resembles that of a monomeric nitroxide-based radical at high fields, dominated by the large anisotropy of the  $g$  and the  $^{14}\text{N}$  hyperfine tensors. Since the overall inhomogeneous spectral width at 140 GHz is  $\Delta \sim 640$  MHz, the CE is the dominant DNP mechanism. In our current DNP instrument, the microwave excitation bandwidth is in the range of a few MHz, and is small compared to the inhomogeneous breadth of the EPR spectrum,  $\Delta$ . Hence, only a small portion of the EPR spectrum is excited by the microwave radiation, corresponding to a particular set of molecular orientations. This phenomenon is referred to as 'orientation selection' and is well known in EPR/ENDOR spectroscopy.[18,19] For nitroxide-based radicals, the orientation selection is facilitated by the large anisotropy of the  $g$ - and the  $^{14}\text{N}$  hyperfine tensor ( $g_{xx} = 2.00980$ ,  $g_{yy} = 2.00622$ ,  $g_{zz} = 2.00220$ ,  $A_{xx} = 17.0$ ,  $A_{yy} = 20.5$ ,  $A_{zz} = 95.9$  MHz for TEMPO [20]). Furthermore, among the excited spins, only those satisfying the matching condition  $\omega_{S1} - \omega_{S2} \approx \pm \omega_{0I}$  contribute significantly to the DNP effect.[9,10] Thus, for an inhomogeneously broadened EPR line with  $\delta > \omega_{0I} > \Delta$ , this two step process (orientation selection and frequency matching) governs the field dependence of the DNP effect.

The field-dependent DNP enhancement profile of bTbk (Figure 4, bottom) shows a maximum positive enhancement at a field position corresponding to 212.058 MHz  $^1\text{H}$  Larmor frequency (DNP(+)) and a maximum negative enhancement at 211.516 MHz (DNP(-)), separated by 542 kHz (357 MHz for  $e^-$ ). The zero crossing occurs at  $\sim 211.8$  MHz coinciding with the maximum absorption in the EPR spectrum ( $g_{yy}$  tensor component of TEMPO).

The DNP enhancement profile recorded for bTbk shows a pronounced asymmetry across the EPR line, conveniently described by the ratio of the maximum negative and positive enhancement  $\varepsilon^-/\varepsilon^+$ , which is 0.62 for bTbk (Figure 4, bottom, solid line). The same asymmetry is observed if the  $^1\text{H}$  polarization is measured through indirect  $^{13}\text{C}$  detection, giving enhancement factors of  $\varepsilon^+ = 250$  and  $\varepsilon^- = 155$  (see Figure 2, insets). This asymmetry

of the enhancement profile observed for bTbk is more pronounced than for previously studied biradicals, including TOTAPOL and BTUrea, for which a smaller asymmetry of  $\epsilon^-/\epsilon^+ = 0.84$  is observed [12] (Figure 4). In addition, other TEMPO based biradicals, such as BT2E showed a similar asymmetry factor of  $\sim 0.8$ , [12] while the DNP enhancement profile for monomeric TEMPO is almost symmetric ( $\epsilon^+/\epsilon^- \sim 1$ ). [21,22] These observations suggest that the origin of the asymmetry is an intrinsic feature of TEMPO based biradicals, and that the extent of the observed asymmetry is a result the flexibility/rigidity of the connecting tether and the relative orientation of the two TEMPO rings. Numerical simulations are currently in progress to investigate this behavior in more detail.

In conclusion, our experiments demonstrate the superior performance of the biradical bTbk when compared to other TEMPO biradicals thus far used in DNP experiments. The enhancement factors obtained with bTbk are about 1.4 times larger than for TOTAPOL under identical experimental conditions. However, due to its limited solubility, bTbk requires the use of a modified solvent matrix with reduced water content. This compromises the DNP efficiency, and limits the applicability of bTbk to biological systems that require glycerol/water matrices. Concurrently, the larger enhancements observed under these suboptimal conditions provides the motivation for the development of H<sub>2</sub>O soluble bTbk derivatives and other polarizing agents with strong  $e^-e^-$  dipole couplings, rigid tethers, and the correct relative orientations of their associated g-tensors.

## Experimental Section

### Synthesis

The biradical bTbk was synthesized in a two-step sequence with 35% overall yield. The bispiketal skeleton was obtained by reacting pentaerythritol (0.87 g, 6.4 mmol) with 2,2,6,6-tetramethyl-4-piperidone (2.00 g, 12.8 mmol) in the presence of *p*-toluenesulfonic acid (2.21 g, 12.8 mmol) in toluene at reflux. The biradical bTbk was obtained as orange crystals by oxidation of the corresponding diamine at 0°C by 1.5 equivalents of MCPBA in CH<sub>2</sub>Cl<sub>2</sub>. Detailed instructions and characterization are provided as supporting information.

### Sample preparation

For DNP experiments 9 mM solutions of bTbk or TOTAPOL in d<sub>6</sub>-DMSO/D<sub>2</sub>O/H<sub>2</sub>O (77/17/6) were prepared. The small amount of H<sub>2</sub>O is required to optimize the diffusion of the local DNP enhanced nuclear polarization to neighboring nuclei, and is held fixed at 6 % for all samples. For matrix studies two more TOTAPOL samples were prepared in d<sub>6</sub>-DMSO/D<sub>2</sub>O/H<sub>2</sub>O (64/30/6) and d<sub>6</sub>-DMSO/D<sub>2</sub>O/H<sub>2</sub>O (50/44/6). The TOTAPOL concentration was held constant at 9 mM in order to facilitate a direct comparison with bTbk. All DNP samples contained 2M <sup>13</sup>C-urea to optimize detection of the NMR signal. The high concentration facilitates observation of the microwave off-signal (no DNP enhancement) in a reasonable time period. For EPR measurements a 2 mM solution of bTbk in DMSO/H<sub>2</sub>O (77/23) was prepared. All solvent mixtures are given in weight percentage.

### DNP experiments

DNP experiments were performed on a custom designed DNP/NMR spectrometer using a triple-resonance cryogenic MAS probe ( $e^-$ , <sup>1</sup>H, and <sup>13</sup>C) with a commercial 2.5 mm rotor stator (Revolution NMR Inc.). The spectrometer operates at a magnetic field of 5 T, corresponding to a Larmor frequency of 140 GHz for  $e^-$  and 211 MHz for <sup>1</sup>H. The enhanced <sup>1</sup>H polarization was indirectly detected, via observation of the cross-polarized <sup>13</sup>C spectrum. The high power microwave radiation is generated by a gyrotron, a vacuum electron device capable of producing high-power (>10 W) millimeter waves, running at a frequency of 139.662 GHz [21,23,24]. The DNP sample is placed in a 2.5 mm sapphire

rotor. Finally, the 5 T superconducting magnet is equipped with a superconducting sweep coil that allows the field to be swept over  $\pm 750$  G to record the DNP field profile and to adjust the magnetic field for maximum enhancements.

### EPR experiments

EPR experiments were performed on a custom designed high field EPR spectrometer described earlier [18,21] running at a microwave frequency of 139.504 GHz. The sample of ~ 250 nL is placed in Suprasil quartz tube of 0.55 mm outer diameter. EPR spectra were recorded using a two-pulse echo sequence ( $\pi/2 - \tau - \pi - \tau - \text{echo}$ ) by integrating the echo intensity while sweeping the magnetic field. Detailed experimental conditions are given in the figure caption. For accurate field measurements the spectrometer is equipped with a field/frequency lock system.[25]

### Supplementary Material

Refer to Web version on PubMed Central for supplementary material.

### References

1. Goertz ST. Nucl. Instrum. Methods Phys. Res., Sect. A. 2004; 526:28.
2. Wind RA, Duijvestijn MJ, d. L. van C, Manenschijn A, Vriend J. Prog. NMR. Spec. 1985; 17:33.
3. Maly T, Debelouchina GT, Bajaj VS, Hu K-N, Joo C-G, MakJurkauskas ML, Sirigiri JR, van der Wel PCA, Herzfeld J, Temkin RJ, Griffin RG. J. Chem. Phys. 2008; 128:052211. [PubMed: 18266416]
4. Barnes AB, De Paëpe G, van der Wel PCA, Hu KN, Joo CG, Bajaj VS, Mak-Jurkauskas ML, Sirigiri JR, Herzfeld J, Temkin RJ, Griffin RG. Appl. Magn. Reson. 2008; 34:237. [PubMed: 19194532]
5. Gallagher FA, Kettunen MI, Day SE, Hu D-E, Ardenkjaer-Larsen JH, Zandt Rit, Jensen PR, Karlsson M, Golman K, Lerche MH, Brindle KM. Nature. 2008; 453:940. [PubMed: 18509335]
6. Hu K-N, Song C, Yu H-h, Swager TM, Griffin RG. J. Chem. Phys. 2008; 128:052302. [PubMed: 18266419]
7. Farrar CT, Hall DA, Gerfen GJ, Inati SJ, Griffin RG. J. Chem. Phys. 2001; 114:4922.
8. Goldman M. Appl. Magn. Reson. 2008; 34:219.
9. Wollan D. Phys. Rev. B. 1976; 13:3671. S.
10. Wollan DS. Phys. Rev. B. 1976; 13:3686.
11. Hu K, Yu H, Swager T, Griffin R. J. Am. Chem. Soc. 2004; 126:10844. [PubMed: 15339160]
12. Song C, Hu K, Joo C, Swager T, Griffin R. J. Am. Chem. Soc. 2006; 128:11385. [PubMed: 16939261]
13. Fujita T, Yoshioka T, Soma N. Journal of Polymer Science: Polymer Letters Edition. 1978; 16:515.
14. Pines A, Gibby MG, Waugh JS. J. Chem. Phys. 1972; 56:1776.
15. Hartmann SR, Hahn EL. Phys. Rev. 1962; 5:2042.
16. Iijima T. Cryobiology. 1998; 36:165. [PubMed: 9597737]
17. Baudot A, Alger L, Boutron P. Cryobiology. 2000; 40:151. [PubMed: 10788314]
18. Bennati M, Farrar C, Bryant J, Inati S, Weis V, Gerfen G, Riggs-Gelasco P, Stubbe J, Griffin R. J. Magn. Reson. 1999; 138:232. [PubMed: 10341127]
19. Schweiger, A.; Jeschke, G. Principles of pulse electron paramagnetic resonance. Oxford, UK: Oxford University Press; 2001.
20. Lebedev, YS.; Grinberg, OY.; Dubinskii, AA.; Poluektov, OG. Bioactive Spin Labels. Zhdanov, R., editor. Heidelberg: Springer Verlag; 1992. p. 227

21. Becerra LR, Gerfen GJ, Bellew BF, Bryant JA, Hall DA, Inati SJ, Weber RT, Un S, Prisner TF, McDermott AE, Fishbein KW, Kreischer K, Temkin RJ, Singel DJ, Griffin RG. *J. Magn. Reson.* 1995; A117:28.
22. Gerfen GJ, Becerra LR, Hall DA, Griffin RG, Temkin RJ, Singel DJ. *J. Chem. Phys.* 1995; 102:9494.
23. Becerra L, Gerfen G, Temkin R, Singel D, Griffin R. *Phys. Rev. Lett.* 1993; 71:3561. [PubMed: 10055008]
24. Granatstein VL, Parker RK, Armstrong CM. *Proc. IEEE.* 1999; 87:702.
25. Maly T, Bryant J, Ruben D, Griffin R. *J. Magn. Reson.* 2006; 183:303. [PubMed: 17027306]

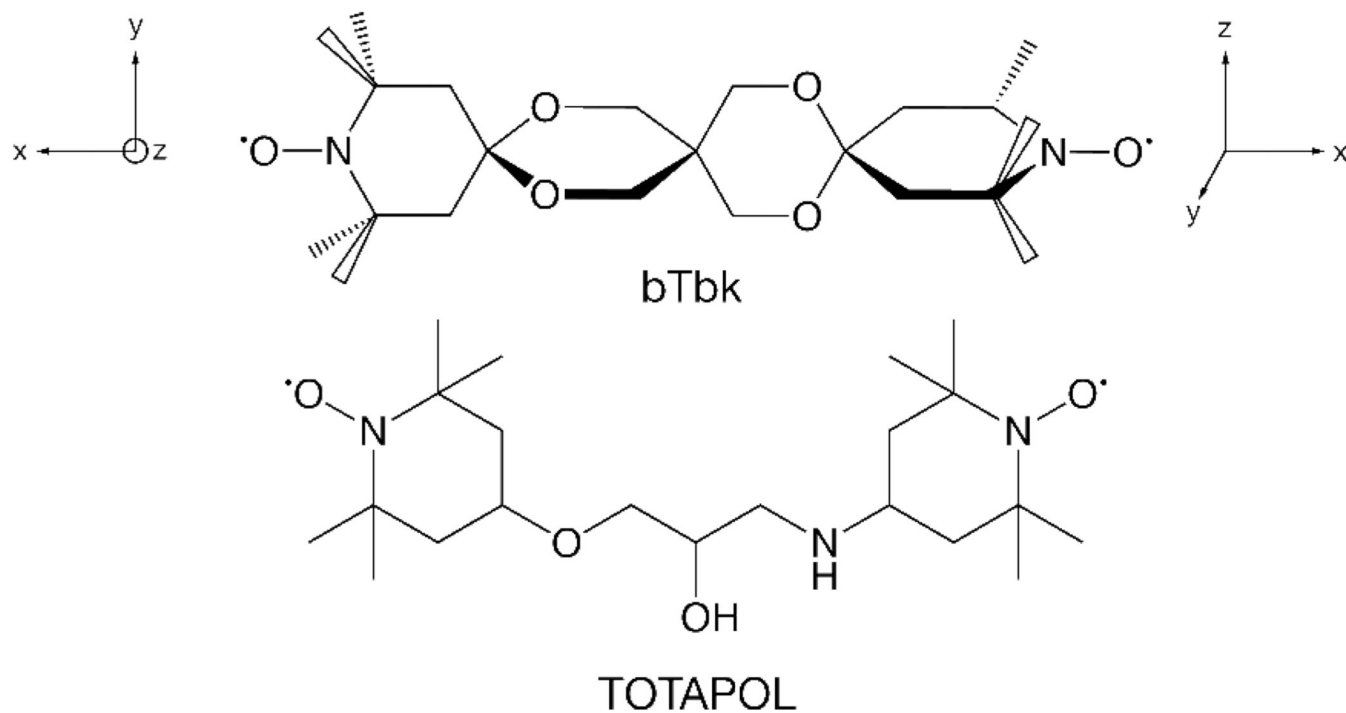


**Figure 1.** Molecular Structure of the two biradicals used in DNP experiments described here. Top: bis-TEMPO-bis-ketal (bTbk). The axis system on each side of the molecule shows the direction of the principal  $g$ -tensor components of TEMPO for the assumed perfect perpendicular relative orientation. Bottom: TOTAPOL.



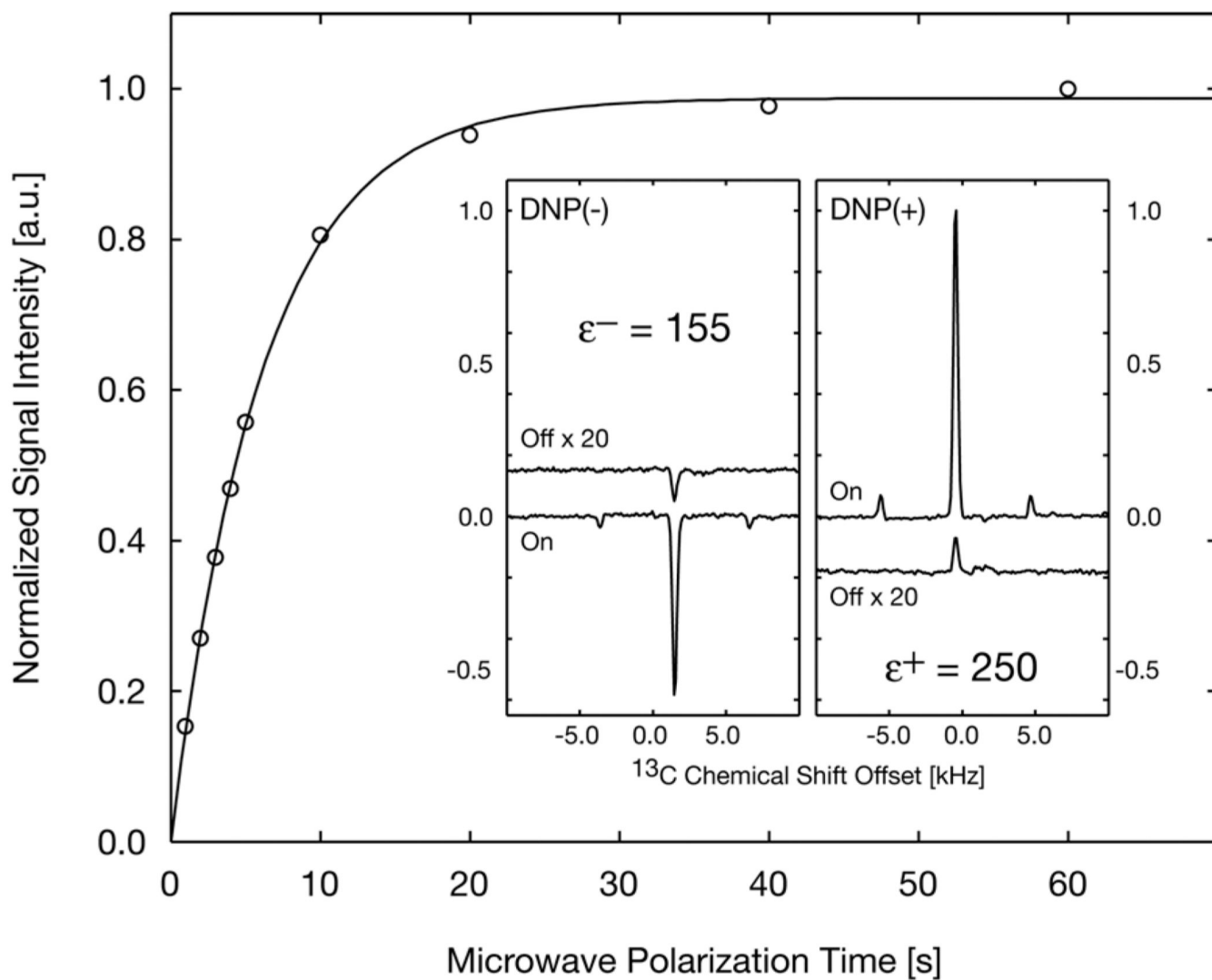


**Figure 2.**

<sup>1</sup>H bulk polarization build-up curve for bTbk recorded at a magnetic field position corresponding to DNP(+). The <sup>1</sup>H polarization is indirectly detected on the <sup>13</sup>C signal of urea via a CP step. The insets show the mw on- and off-signal recorded at field positions corresponding to DNP(+) and DNP(-), T = 94 K,  $\omega_p/2\pi = 4.8$  kHz.

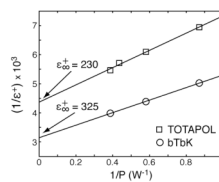


**Figure 3.** Power dependence of the steady-state DNP enhancement ( $\epsilon^+$ ) for bTbk and TOTAPOL, recorded under similar experimental conditions.

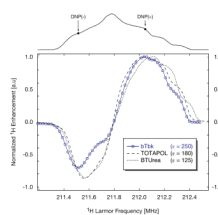


**Figure 4.**

Field dependence of the DNP enhancement profiles and EPR spectrum of bTbk. Top: 140 GHz echo detected EPR spectrum of bTbk in DMSO/H<sub>2</sub>O (77/23), T = 20 K,  $t_p(\pi/2) = 60$  ns,  $\tau = 300$  ns. Bottom: <sup>1</sup>H detected DNP field profile of bTbk (solid line), TOTAPOL (dashed line), and BTUrea (dotted line). T = 94 K,  $t_p(\pi/2) = 3$   $\mu$ s,  $\omega_r/2\pi = 4.8$  kHz. All three enhancement profiles were recorded under similar experimental conditions and are normalized to the maximum positive enhancement. The individual data points are included for bTbk but similar data were recorded for TOTAPOL and BTUrea. The points are not included on the plot to permit the curves to be easily distinguished. Enhancement factors for bTbk, TOTAPOL and BTUrea under optimal experimental conditions are given in the box.

**Table 1**

DNP enhancements at infinite microwave powers for different TEMPO based biradicals

| Biradical               | $\epsilon_{\infty}$ | Biradical                   | $\epsilon_{\infty}$ |
|-------------------------|---------------------|-----------------------------|---------------------|
| BT2E [ <sup>a</sup> ]   | 260                 | BTOXA [ <sup>a</sup> ]      | 70                  |
| BT3E [ <sup>a</sup> ]   | 175                 | TOTAPOL [ <sup>a, b</sup> ] | 260                 |
| BT4E [ <sup>a</sup> ]   | 105                 | TOTAPOL [ <sup>c</sup> ]    | 230                 |
| BTUrea [ <sup>a</sup> ] | 205                 | bTbk [ <sup>c</sup> ]       | 325                 |

[<sup>a</sup>] Values taken from [6], d<sub>6</sub>-DMSO/D<sub>2</sub>O/H<sub>2</sub>O (60/34/6), T = 90 K.

[<sup>b</sup>] The previously published value is incorrect and the correct values is given here.

[<sup>c</sup>] Measurements presented here, d<sub>6</sub>-DMSO/D<sub>2</sub>O/H<sub>2</sub>O (77/17/6), T = 93 K.